PHYSICAL REVIEW B VOLUME 51, NUMBER 10 1 MARCH 1995-II

Measurements of the dc Josephson current in proximity systems

C. Camerlingo, R. Monaco, B. Ruggiero, and M. Russo
Istituto di Cibernetica del Consiglio Nazionale delle Ricerche, I-80072 Arco Felice (Napoli), Italy

G. Testa
Istituto Nazionale di Fisica Nucleare, I-80125 Napoli, Italy
(Received 24 October 1994)

Junctions modeled as S-$N/I/S$ and S-$N/I/N$-S proximity systems (where S, I, and N indicate a superconductor, an insulator, and a normal metal, respectively) are widely discussed in literature from both the experimental and theoretical point of view. In the present paper experimental aspects concerning Nb/Nb junctions including a proximity bilayer are considered. Nb-M/I/Nb and M-Nb/I/Nb structures (where M is a normal metal, a semimetal, or a superconductor) are investigated by using a semimetal (bismuth) and a superconductor (aluminum) as the M layer. In particular, how the deposition of a back layer influences the behavior of Nb/I/Nb high-quality junctions is discussed, focusing the interest on measurements of the temperature dependence of the maximum dc Josephson current. Experimental data are discussed in the framework of Kresin's theoretical calculations based on the thermodynamic Green's function method.

I. INTRODUCTION

The presence of proximity systems in superconducting tunnel junctions is a widely investigated topic from both the experimental and theoretical point of view.[1] More recently, its role in determining the quality of all refractory Nb/Nb Josephson junctions has promoted experimental investigations.[2] The results have been discussed in the framework of theoretical models available in literature[3–8] generally referring to the McMillan one.[4] However, in spite of a large interest in $S/I/N$-S and S-$N/I/N$-S structures (S and N are a superconductor and a normal metal, respectively), there is a lack of information about tunnel junctions in which the proximity effect occurrence is related to the presence of a normal metal layer on the back of one of the two superconducting electrodes (back layer). Experiments on this kind of structures were performed[9] since 1979 and their behavior was discussed, near the critical temperature T_c, in the framework of the de Gennes approach.[3]

More recently, experiments were proposed by Kresin[10] in order to study the effect of semimetal back layers. This proposal was discussed in the framework of a theoretical approach to Josephson tunnel junctions including proximity systems just developed by the same author,[6] this being a more general approach than the McMillan one.

In the present paper, the occurrence of proximity effects in Josephson tunnel junctions is experimentally investigated, focusing attention on the temperature dependence of the dc Josephson current, I_c vs T, in structures having a back layer. Proximity systems constituted by quite thin films have been considered to investigate the feasibility of observations of normal layer properties (e.g., self-quantization and structural transitions) by Josephson junctions. Different kinds of back layers, including normal metals, superconductors, semiconductors, and semimetals, have been deposited onto high-quality Nb/Nb all refractory junctions. In particular, data concerning junctions with back layers by aluminum and bismuth are reported. In order to distinguish the effects due to such layers from those ones coming from an incomplete oxidation of the aluminum barrier film, which leads to the formation of a proximity system, careful control of the fabrication process has been maintained. So, back layers have been deposited only on samples exhibiting no evidence of proximity coming from the barrier layer (this point shall be better discussed in the following). The experimental data are compared with calculations performed in the framework of Kresin's theoretical approach[6] to Josephson tunneling in junctions including a S-M proximity system (M is either a normal metal or a superconductor with a transition temperature $T_{cM} < T_{cS}$) on either one or both sides of the barrier. Such an approach is based on the thermodynamic Green's function method, and it supplies calculations of the $I_c(T)$ taking into account the presence of a back layer and strong coupling effects. The description of the M-S inhomogeneous system is carried out starting from the McMillan tunneling approach to proximity effect[4] including the electron-phonon interaction.[11] In this framework the layers S and M have to be considered as separated from each other by a potential barrier having a transmission probability $\sigma \ll 1$, S is assumed to be "dirty" in the Anderson sense,[12] and the coupling between the two layers is characterized by the parameter $\Gamma_{M(S)} = \hbar v_{FM(S)} \sigma / 2B d_{M(S)}$ where v_F is the Fermi velocity and B is a function of the ratio between the electron mean free path and the film thickness d. Compared to the McMillan model, Kresin's needs the less restrictive conditions on the film thicknesses $d_M \ll \xi_M$ and $d_M < d_S$, ξ being the coherence length. An exhaustive discussion on the theoretical aspects can be found in Refs. 6, 11, and 13. Limiting the attention to junctions which can be modeled as M-$S/I/S$ and

S-$M/I/S$ structures, calculations of $I_c(T)$ have been carried out for the following three cases.

A. S_α-$S_\beta/I/S_\gamma$ structure

This case refers to a junction in which the M layer is a weak coupling superconductor S_β with $T_{c\beta} < T_{c\alpha}$.

The temperature dependence of the maximum dc Josephson current is

$$I_C(T) = \frac{2\pi k_B T}{eR_N} \frac{\varepsilon_\gamma(T)}{\varepsilon_\alpha(T)} \sum_{n \geq 0} S_n(T,t) , \tag{1}$$

where k_B and e have the usual meaning, R_N is the tunneling resistance, $\varepsilon_{\alpha(\gamma)}$ the energy gap, n is an integer, $t = \pi k_B T_{c\alpha}/\Gamma_\beta(1+\lambda_\beta)$, λ_β being the electron-phonon interaction constant, and S_n is

$$S_n = \frac{f_\alpha(x_n) + \delta t k(x_n)}{\{x_n^2[1+tk(x_n)]^2 + [f_\alpha(x_n)+\delta t k(x_n)]^2\}^{1/2}} \times \frac{f_\gamma(x_n)}{\{x_n^2 + [\varepsilon_\gamma^2(T)/\varepsilon_\alpha^2(T)] f_\gamma^2(x_n)\}^{1/2}} \tag{2}$$

with

$$\delta = \frac{\lambda_\beta \pi k_B T}{(1+\lambda_\beta)\varepsilon_\alpha(T)} \sum_{n \geq 0} \frac{S_n(T,t)\mu_\beta}{f_\gamma(x_n)/\{x_n^2 + [\varepsilon_\gamma^2(T)/\varepsilon_\alpha^2(T)] f_\gamma^2(x_n)\}^{1/2}} \tag{3}$$

$$\mu_\beta = \frac{\hbar^2 \Omega_\beta^2}{\hbar^2 \Omega_\beta^2 + x_n^2 \varepsilon_\alpha^2(T)} , \tag{4}$$

$$x_n = \frac{(2n+1)\pi k_B T}{\varepsilon_\alpha(T)} , \tag{5}$$

$$f_{\alpha(\gamma)}^{-1}(x_n) = 1 + [x_n \varepsilon_{\alpha(\gamma)}(T)/\hbar\Omega_{t\alpha(\gamma)}]^2 , \tag{6}$$

$$k(x_n) = [\varepsilon_\alpha(T)/\pi k_B T_c^\alpha][x_n^2 + f_\alpha^2(x_n)]^{1/2} . \tag{7}$$

Here $\hbar\Omega_\beta$ and $\hbar\Omega_{t\alpha(\gamma)}$ are the energy values corresponding to the Debye frequency and to the transverse branch in the phonon spectrum of the superconductor, respectively.

It is worth noting that strong coupling effects on the normalized order parameter $\Delta_{\alpha(\gamma)}/\varepsilon_{\alpha(\gamma)} = f_{\alpha(\gamma)}$ are considered by Eq. (6); for a weak coupling electron-phonon interaction the value of $f_{\alpha(\gamma)}$ reduces to 1.

Obviously if $f_\alpha = f_\gamma = 1$ and $t=0$, Eq. (1) gives the same $I_c(T)$ dependence calculated for a $S_\alpha/I/S_\gamma$ junction by Ambegaokar and Baratoff.[14]

B. S_α-$N/I/S_\gamma$ structure

This is a limit case of the previous one for $T_{c\beta}=0$. M is a normal metal (i.e., $\lambda_\beta = 0$) so that $\delta=0$. The temperature dependence of the maximum dc Josephson current is still given by Eq. (1) with

$$S_n = \frac{f_\alpha(x_n)}{\{x_n^2[1+tk(x_n)]^2 + f_\alpha^2(x_n)\}^{1/2}} \times \frac{f_\gamma(x_n)}{\{x_n^2 + [\varepsilon_\gamma^2(T)/\varepsilon_\alpha^2(T)] f_\gamma^2(x_n)\}^{1/2}} . \tag{8}$$

C. N-$S_\alpha/I/S_\gamma$ structure

In such a case it is

$$I_C(T) = \frac{2\pi k_B T}{eR_N} \sum_{n \geq 0} \frac{1}{[1+x_n^2(T)]^{1/2}\{1+[\varepsilon_\alpha^2(T)/\varepsilon_\gamma^2(T)]x_n^2(T)\}^{1/2}} - \frac{2\pi k_B T \Gamma_\alpha}{(1+\lambda_\alpha)eR_N\varepsilon_\alpha(T)} \sum_{n \geq 0} \frac{x_n^2(T)/[1+x_n^2(T)]}{\{x_n^2(T)[1+x_n^2(T)+\gamma^2]\}^{1/2}\{1+[\varepsilon_\alpha^2(T)/\varepsilon_\gamma^2(T)]x_n^2(T)\}^{1/2}} \tag{9}$$

with $\gamma = \Gamma_N/\varepsilon_\alpha(T)$. Equation (9) is obtained in weak coupling approximation and in the limit $\Gamma_N, \Gamma_\alpha \ll \varepsilon_\alpha(T)$.[10,15] It is easy to verify that for $\Gamma_\alpha \to 0$ (either $d_{S\alpha} \gg \xi_\alpha$ or $\sigma \to 0$) and $\Gamma_N \to \infty$ $(d_N \to 0)$ the $I_c(T)$ reduces to the expression for a $S_\alpha/I/S_\gamma$ structure. Since a typical procedure to compare theory and experiments uses normalized $I_c(T)/I_c(0)$ dependences, the $I_c(0)$ value can be easily evaluated from the above reported equations by substituting

$$\int dx \quad \text{for} \quad [2\pi k_B T/\varepsilon_\alpha(0)] \sum_n .$$

II. EXPERIMENTAL PROCEDURES

A. Sample fabrication

All the experiments considered in the present paper are dealing with structures based on Nb-Al/AlOx/Nb high-quality junctions. Their fabrication is widely described elsewhere,[16] so only an outline of the procedure is reported here together with details of the steps involved in the formation of the *S*-*M* proximity bilayers.

The samples have been fabricated on 7059 Corning glass substrates. The basic Nb-Al/AlOx/Nb structure has been obtained from a trilayer formed *in situ* by rf magnetron sputtering in an argon atmosphere. The tunneling barrier is obtained by thermal oxidation of the aluminum layer in a pure oxygen atmosphere for 1 hour at room temperature. Some fabrication parameters are summarized in Table I. Obviously different aluminum thicknesses have to be used to get junctions which can be modeled as $S/I/S$, $S/I/S$-M or $S/I/M$-S structures. In order to neglect any contribution to the critical current from the proximity effect in the aluminum layer, its thickness has to be of the order of a few nanometers. So values of $d_{\rm Al} \leq 3$ nm have been considered. Furthermore it is worth noting that the thickness of the top niobium layer is comparable with its coherence length ($\xi_\alpha = 40$ nm) to allow a better observation of the effects due to the back layer. This circumstance together with a further thinning of the top niobium film performed before the back layer deposition leads to a lowering of the critical temperature $T_{c\alpha}$; so the two niobium electrodes have to be generally regarded as different superconductors. Standard photolitography techniques, reactive ion etching in $CF_4+O_2(5\%)$ rf plasma (for Nb) and a wet etching in dilute H_3PO_4 at 80 °C (for Al and AlOx) are used to pattern the whole trilayer. The junction geometry is obtained by a selective niobium anodization process (SNAP).

On each substrate there are six junctions having a $(50\times 50)\ \mu\text{m}^2$ square geometry with a small tail for electrical connection to the top layer, its area is less than 3% of the total one. As a final step a niobium film (150 nm thick) is deposited and patterned by a lift-off process to provide the proper wiring. It is worth noting that the wiring covers only the tail area.

At this stage the basic structures ($S_\alpha/I/S_\gamma$ and S_α-$S_\beta/I/S_\gamma$ like) are ready for low-temperature measurements. Samples in which the proximity effect due to the aluminum layer is negligible can be processed afterwards to deposit a back layer ($S_\gamma/I/S_\alpha$-M). The fabrication procedure consists in the deposition of the *M* layer just after a soft sputter cleaning of the top niobium electrode without breaking the vacuum. This procedure is carried out in an UHV vacuum system equipped with a rf back sputtering station and a 2 kW three crucible electron gun source. The samples are mounted on a 12.7 cm cathode and sputtered in an argon atmosphere ($p_{\rm Ar}=3.5$ mTorr) at a peak to peak voltage $V_{\rm rf}=500$ V corresponding to an etching rate $r \approx 1.3$ nm/min. Typically about 10 nm of niobium are etched to get a clean surface without a detectable degradation of the insulating layer. After the cleaning process the back layer is deposited by the *e*-gun source; the initial pressure is in the 10^{-8} Torr range. The film geometry is defined by an aluminum stencil mask.

B. Experimental technique

The junctions are investigated down to a limiting temperature of about 1 K in a He^4 cryostat connected to a Roots pump. Temperatures above 4.2 K are achieved allowing a slow cooling down of the sample by carefully controlling its distance from the helium bath by a suitable mechanical device. To improve temperature stability the samples are mounted on a copper block. Temperature values below 4.2 K are achieved by regulating the helium vapor pressure by a manostat. The temperature is measured by a Lake Shore 820 cryogenic thermometer with a germanium sensor in close contact with the junction, the overall accuracy being better than 0.01 K.

The whole cryostat is shielded by three μ-metal cans and a copper one. An external magnetic field is provided by a long solenoid (0.986 G/mA) surrounding the junctions.

The current-voltage characteristics of the junctions are displayed on a HP 7090A plotting system and careful measurements of the maximum dc Josephson current are performed by a differential comparator using a Tektronics 7630 x-y oscilloscope. The maximum error in the normalized current measurements is less than 0.005.

For each junction, together with the $I_c(T)$ dependence, the current-voltage characteristics *I*-*V* and magnetic field dependence $I_c(H)$ are measured at $T=4.2$ K and $T=1.2$ K. All the junctions considered exhibit only small deviations from a Fraunhofer-like $I_c(H)$ as expected for their exotic geometrical configuration. Moreover the measurements performed at $T=1.2$ K guarantee substantial uni-

TABLE I. Main fabrication parameters of the Nb-Al/AlOx/Nb trilayers used as basic tunneling structures.

Layer	p (Ar) [mbar]	Dep. rate [nm/s]	Thickness [nm]	p (O_2) [mbar]
First Nb	7×10^{-3}	1.5	200–300	
Al	5×10^{-3}	0.2	3–5[a]	
AlOx				0.1–50[b]
Second Nb	7×10^{-3}	1.5	20–40	

[a]These values refer to trilayers exhibiting a $S/I/S$-like behavior (Ref. 14).
[b]This range of oxygen pressure value leads to critical current densities within 500 and 50 A cm^{-2}.

formity of the critical current density and junction normalized dimensions $L/\lambda_j \leq 1$, λ_j being the Josephson penetration depth.

III. EXPERIMENTAL RESULTS AND DISCUSSION

As previously discussed, different sets of measurements have been carried out following the procedure reported in Sec. II B. A first set is dealing with Nb-Al/AlOx/Nb junctions having different aluminum thicknesses ($2 < d_{\rm Al} < 30$ nm). To identify the junction parameters leading to negligible proximity effect contributions to the $I_c(T)$ dependence, measurements have been compared with Kresin's calculations assuming a S_α-$S_\beta/I/S_\gamma$ model, see Sec. I A. This analysis has shown that junctions with $d_{\rm Al} < 3$ nm can be modeled as a "pure" $S_\alpha/I/S_\gamma$ structure and their $I_c(T)$ can be compared with the Ambegaokar and Baratoff calculations.[14]

This chance of obtaining $S_\alpha/I/S_\gamma$ junctions by a suitable choice of the fabrication parameters, allows one to investigate Josephson structures including a back layer. Data concerning the $I_c(T)$ dependence in presence of a back layer by bismuth and aluminum are compared with Kresin's calculation for a M-$S/I/S$ structure, see Sec. I. In such an analysis two different experimental procedures are followed. The former concerns measurements on the same sample performed before and after the back layer deposition. The latter involves a comparison of M-$S/I/S$ samples with junctions on their own substrate with $d_M = 0$. The adoption of both procedures better clarify the role of the M layer in the junction behavior.

A. Nb-Al/AlOx/Nb junctions

To investigate the effect of the aluminum barrier layer on the $I_c(T)$ dependence of a Nb/Nb junction and to compare the experimental results with the theoretical behavior described by Eq. (1), structures with an aluminum thickness in the range 10–30 nm have been considered. It is worth noting that the reported $d_{\rm Al(Nb)}$ are effective values as evaluated by the anodization spectroscopy technique.[17]

In Fig. 1 a typical experimental $I_c(T)/I_c(0)$ dependence is reported. It refers to a sample having $d_{\rm Al} = 13 \pm 2$ nm, $d_{{\rm Nb}\alpha} \approx 200$ nm, and $d_{{\rm Nb}\gamma} \approx 40$ nm. For a comparison between experimental data and theory, independent measurements of T_c and ε for both niobium layers are performed. The same $2\varepsilon/k_B T_c$ ratio in the two electrodes is assumed. As expected the experimental $I_c(T)$ dependence clearly disagrees with the behavior calculated by Ambegaokar and Baratoff for a $S_\alpha/I/S_\gamma$ junction. To compare the data with the behavior computed by Eq. (1), tabulated values for λ_β, Ω_D, and Ω_t have been employed using t as a free parameter. A best-fitting procedure to the experimental data allows its evaluation which turns in the evaluation of $\Gamma_{\rm Al}$ and σ. For the sample reported in Fig. 1 a best-fitting value $t = 1.05$ corresponding to $\Gamma_{\rm Al} = 1.66$ meV is obtained. From this result, by using a tabulated value of v_F, the measured thickness $d_{\rm Al}$, and $B = 2$, $\sigma = 0.06$ is estimated; this value

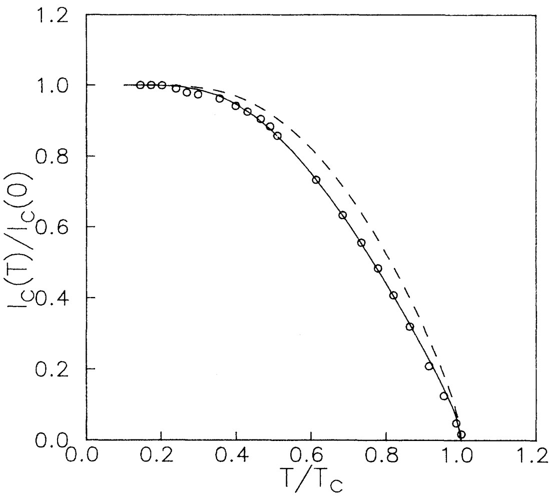

FIG. 1. Normalized temperature dependence of the maximum dc Josephson current for a Nb-Al/AlOx/Nb tunnel junction. The experimental data (circles) refer to a sample having a "thick" aluminum layer ($d_{\rm Al} = 13$ nm), see text. The solid curve is the theoretical behavior computed by Eq. (1); the value of the best-fitting parameter is $t = 1.05$. The theoretical behavior (dashed line) obtained following the Ambegaokar and Baratoff calculations (Ref. 14) is also reported for comparison.

is in agreement with the theoretical hypothesis $\sigma \ll 1$. Generally speaking all the experimental $I_c(T)$ data are well accounted in the framework of Kresin's calculations. As previously discussed, a suitable choice of the aluminum layer thickness ($d_{\rm Al} \leq 3$ nm) allows junctions exhibiting negligible proximity effect. A reduction of $d_{\rm Al}$ leads to an $I_c(T)$ dependence undistinguishable from the Ambegaokar and Baratoff behavior. This circumstance is reported in Fig. 2 where experimental data and calculations for a $S_\alpha/I/S_\gamma$ structure are shown. Data refer to a junction having $d_{\rm Al} \approx 3$ nm, $d_{{\rm Nb}\alpha} \approx 200$ nm, and $d_{{\rm Nb}\gamma} \approx 40$ nm. In computing the theoretical behavior, experimental evaluations of the tunneling resistance R_N, $T_{c{\rm Nb}\alpha(\gamma)}$, and energy gap $\varepsilon_{\alpha(\gamma)}$ have been used. An excellent agreement between theory and experiment has been found although a very small tail is observable near T_c as an effect of the niobium wiring. It is worth noting that effects due to the wiring mainly depend on junction geometry (contact area) and on fabrication parameters such as $d_{{\rm Nb}\gamma}$ and $d_{\rm Nb\ wiring}$, so their relevance can be easily modified. For instance, their enhancement is shown in Fig. 3 as the occurrence of a further gap structure clearly detectable in the I-V characteristics. A quantitative discussion of such an observation shall be reported in a furthercoming paper mainly devoted to more detailed measurements of the I-V characteristics.

B. M-Nb/AlOx/Nb junctions

The feasibility of junctions exhibiting no evidence of proximity effect in the $I_c(T)$ dependence makes them suitable to investigate the influence of an additional M layer. In particular junctions with a niobium film thick-

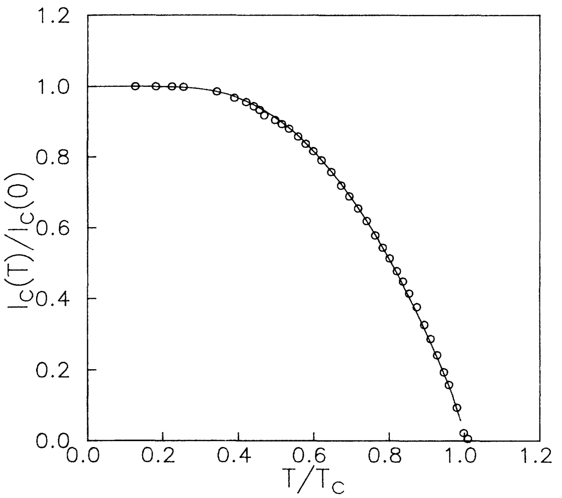

FIG. 2. Normalized temperature dependence of the maximum dc Josephson current for a Nb/Nb sample having $d_{\mathrm{Al}}=3$ nm. The experimental data (circles) are compared with the theoretical behavior (solid line) for a Nb/AlOx/Nb junction. The very good agreement between the experimental behavior and the Ambegaokar and Baratoff calculations (Ref. 14) justifies the assumption that a small d_{Al} allows an almost complete oxidation of the layer making negligible the occurrence of proximity effect.

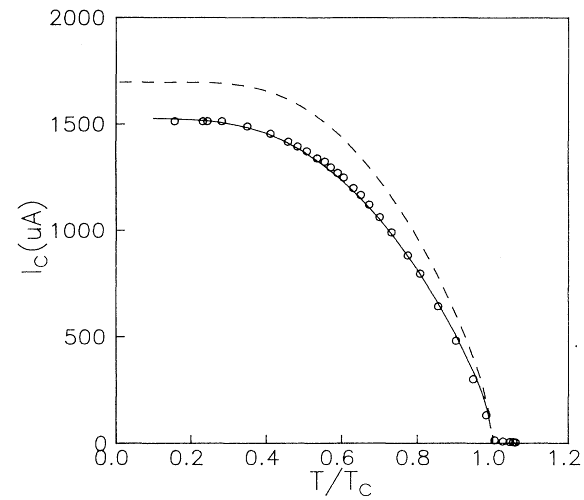

FIG. 4. Temperature dependence of the maximum dc Josephson current in a Bi-Nb/AlOx/Nb junction. The back layer has a thickness $d_{\mathrm{Bi}}=20$ nm. The experimental data (circles) are compared with the theoretical behavior calculated by Ambegaokar and Baratoff (Ref. 14) for a $S_\alpha/I/S_\gamma$ junction (dashed curve). By a one-parameter best-fitting procedure the experimental data are also compared with the behavior of a N-$S_\alpha/I/S_\gamma$ structure following Eq. (9) (solid curve).

ness thin enough ($d_{\mathrm{Nb}\alpha}\leq\xi_{\mathrm{Nb}}$) to allow a clear observation of the proximity effect are considered (very thin films would lead to a severe depression of both critical temperature and energy gap). Structures with a M layer of bismuth, having a thickness ranging from 20 to 150 nm, have been considered. Compared to samples measured before the back layer deposition, general features of the Bi-Nb/AlOx/Nb junctions are reduced values of ε_α, T_c, and $I_{c\max}$ together with a substantially constant value of R_N. Moreover the experimental I_c vs T dependence disagrees with the behavior computed in the framework of the Ambegaokar and Baratoff theoretical approach. This circumstance is clearly shown in Fig. 4 which refers to a Bi-Nb/AlOx/Nb junction having $d_{\mathrm{Bi}}=20$ nm. The

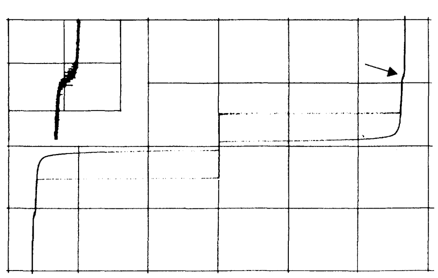

FIG. 3. Current-voltage characteristics of a Nb/Nb junction at $T=4.2$ K and $H\neq0$. The occurrence of a double gap structure due to the wiring layer is exhibited. Vertical scale: 5 mA/div; horizontal scale: 1 mV/div. In the inset the scales are magnified 5× and 10×, respectively.

experimental data (circles) are far from the theoretical curve (dashed curve) calculated by taking into account the depressed values of ε_α and $T_{c\alpha}$. The interpretation of the experimental behavior in the framework of proximity effect in the Bi-Nb bilayer is justified by the very good agreement with the dependence computed for a N-$S_\alpha/I/S_\gamma$ structure, see Eq. (9), using the same best-fitting procedure described above, with $\Gamma_{\mathrm{Nb}\alpha}$ and Γ_{Bi} as free parameters. In practice, by measuring d_{Nb} and d_{Bi}, the two parameters can be easily related because $\sigma_{\mathrm{Bi}}=\sigma_{\mathrm{Nb}\alpha}$ and $I_c(T)$ depend on Γ_{Bi} very weakly. So Eq. (9) reduces from a two parameter to a one parameter expression. For the sample considered, a very good agreement between measurements and theory (solid curve) has been found for $\Gamma_{\mathrm{Nb}}=0.82$ meV, corresponding to $\sigma=0.09$.

A similar experimental behavior is also observed for samples having a rather thick bismuth layer. Such a case is reported in Fig. 5, referring to the same sample considered in Fig. 2 after the deposition of a 150-nm thick bismuth layer. A remarkable discrepancy between the experimental behavior (circles) and Ambegaokar and Baratoff calculations (dashed curve) is clearly exhibited. In this case, a quantitative analysis of the experimental data cannot be performed since d_{Bi} is not within the limits of Kresin's calculations and Eq. (9) itself is strictly valid only for thin normal layer. In spite of these considerations, in the figure is shown the theoretical dependence (solid curve) computed for a value of the best-fitting parameter $\Gamma_{\mathrm{Nb}\alpha}=0.55$ meV corresponding to $\sigma=0.06$.

It is worth noting that, near T_c, in both the experimen-

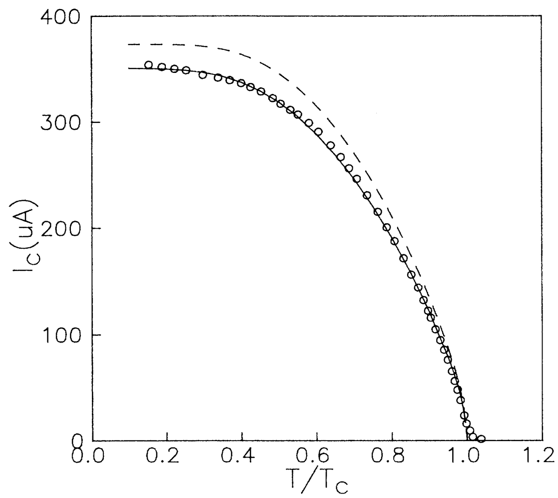

FIG. 5. Temperature dependence of the maximum dc Josephson current in a Bi-Nb/AlOx/Nb junction. The sample is the same as Fig. 2 but after the deposition of a 150-nm thick bismuth layer. The experimental data (circles) are compared with the theoretical behavior calculated by Ambegaokar and Baratoff (Ref. 14) for a $S_\alpha/I/S_\gamma$ junction (dashed curve). Though improperly, the experimental data are compared with the behavior of a N-$S_\alpha/I/S_\gamma$ structure (solid curve) by the same procedure used in Fig. 4.

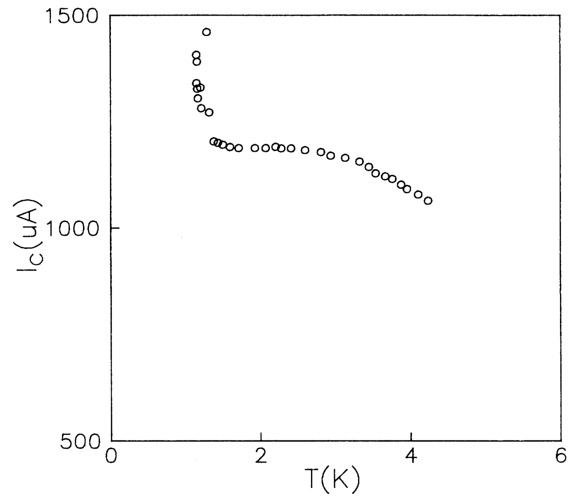

FIG. 6. Temperature dependence of the maximum dc Josephson current in an Al-Nb/AlOx/Nb junction at temperatures below 4.2 K. The aluminum back layer has a thickness $d_{\mathrm{Al}}=150$ nm. Present calculations in the framework of Kresin's theoretical approach cannot account for the superconducting properties of the back layer.

tal $I_c(T)$ dependences reported, the effect of the niobium wiring is still observable as a tail. In comparison with the data reported in Fig. 2, a longer tail is exhibited. This circumstance is mainly due to the reduction of $d_{\mathrm{Nb}\alpha}$ (turning into a T_c reduction) caused by the back-sputtering process, see Sec. III.

The agreement between theory and experiments supports the chance of observing the possible occurrence of size quantization and structural transition[18] in the bismuth layer by I_c measurements, as suggested by Kresin.[10] To this purpose both measurements of $I_c(T)$ in junctions with $d_{\mathrm{Bi}}<20$ nm and the dependence $I_c(d_{\mathrm{Bi}})$ have to be carefully performed. Moreover improvements in the bismuth deposition process have to be carried out. So, from this point of view, the experiments discussed here have to be considered as incomplete and, consequently, no clear evidences of the two effects have been detected.

Finally, although theoretical calculations do not yet account for possible superconducting properties of the M layer, experiments have been carried out using aluminum films as back layers. Preliminary measurements at temperatures $T\leq 4.2$ K on a Al-Nb/AlOx/Nb with $d_{\mathrm{Al}}\approx 150$ nm are reported in Fig. 6. As clearly shown in the figure, the hallmark feature of the I_c vs T dependence is a fast increase of the Josephson current at a temperature $T^*=1.59$ K near $T_{c\mathrm{Al}}=1.18$ K, the aluminum bulk critical temperature. This rise is due to the variation of the order parameter in the niobium top electrode related to the normal-superconductor transition of the M layer at a temperature $T^*>T_{c\mathrm{Al}}$ as expected for the influence of the niobium electrode itself. Theoretical calculations are in progress to quantitatively account for such an experimental behavior.

IV. CONCLUSIONS

Proximity effect in different kinds of superconducting tunnel structures have been considered. Fabrication processes have been developed to get high-quality all refractory niobium junctions with a top electrode thin enough ($d_{\mathrm{Nb}}<\xi_{\mathrm{Nb}}$) to investigate the influence on their behavior of normal and superconducting ($T_c<T_{c\mathrm{Nb}}$) layers either inside or outside the junction trilayer. Nb-Al/AlOx/Nb, Bi-Nb/AlOx/Nb, and Al-Nb/AlOx/Nb junctions have been experimentally investigated. In particular the temperature dependence of the maximum dc Josephson current has been considered referring to Kresin's theoretical approach based on the thermodynamic Green's function method. Its interest lies in the less restrictive conditions on the film thicknesses compared to other approaches, in the possibility of taking into account strong coupling superconductors, and in less tedious calculations. In this framework, a comparison between experiments and theory has been performed. A fairly good agreement has been found using Γ as best fitting parameter.

Presently, a lack in the theoretical calculations does not allow any comparison for S_β-$S_\alpha/I/S_\gamma$ (with $T_{c\beta}<T_{c\alpha}$) structures although work is in progress with this aim. It would be also interesting to perform further measurements on structures involving a wider range of film thicknesses and different normal layers.

ACKNOWLEDGMENTS

The authors are grateful to V. Z. Kresin for useful discussions and suggestions. This work was partially supported by the Consiglio Nazionale delle Ricerche under the Progetto Finalizzato "Superconductive and Cryogenic Technologies."

[1]A. Barone and G. Paternò, *Physics and Applications of the Josephson Effect* (Wiley, New York, 1982).
[2]S. Morohashi and S. Hasuo, J. Appl. Phys. **61**, 4835 (1987).
[3]P. G. de Gennes, Rev. Mod. Phys. **36**, 225 (1964).
[4]W. McMillan, Phys. Rev. **175**, 537 (1968).
[5]E. L. Wolf and G. B. Arnold, Phys. Rep. **91**, 31 (1982); G. B. Arnold, J. Low Temp. Phys. **59**, 143 (1985).
[6]V. Z. Kresin, Phys. Rev. B **28**, 1294 (1983).
[7]A. A. Golubov and M. Yu. Kupriyanov, J. Low. Temp. Phys. **70**, 83 (1988).
[8]A. A. Golubov, M. A. Gurvitch, M. Yu. Kupriyanov, and S. V. Polonskii, Zh. Eksp. Teor. Fiz. **103**, 1851 (1993) [Sov. JETP **76**, 915 (1993)].
[9]F. Dettman and G. Albrecht, Phys. Status Solidi A **53**, 541 (1979).
[10]V. Z. Kresin, in *Josephson Effect: Achievements and Trends,* edited by A. Barone (World Scientific, Singapore, 1985), p. 198.
[11]V. Z. Kresin, Phys. Rev. B **25**, 157 (1982).
[12]P. Anderson, Phys. Chem. Solids **11**, 20 (1959).
[13]V. Z. Kresin, Phys. Rev. B **32**, 145 (1985).
[14]V. Ambegaokar and A. Baratoff, Phys. Rev. Lett. **10**, 486 (1963); errata, Phys. Rev. Lett. **11**, 104 (1963).
[15]V. Z. Kresin (private communication).
[16]R. Monaco, R. Cristiano, L. Frunzio, and C. Nappi, J. Appl. Phys. **71**, 1888 (1992).
[17]T. Inamura and S. Hasuo, J. Appl. Phys. **66**, 2173 (1989).
[18]V. Z. Kresin, J. Low. Temp. Phys. **57**, 549 (1984).